Spectrally Sharp Near-Field Thermal Emission: Revealing Some Disagreements between a Casimir-Polder Sensor and Predictions from Far-Field Emittance

J. C. de Aquino Carvalho,[1,†] I. Maurin,[1] P. Chaves de Souza Segundo,[1,‡] A. Laliotis,[1] D. de Sousa Meneses,[2] and D. Bloch[1,*]

[1]*Laboratoire de Physique des Lasers, UMR 7538 du CNRS, Université Sorbonne Paris Nord, 99 av. JB Clément, 93430 Villetaneuse, France*

[2]*CNRS, CEMHTI UPR 3079, Université d'Orléans, F-45071 Orléans, France*

(Received 6 December 2021; accepted 1 August 2023; published 2 October 2023)

Near-field thermal *emission* largely exceeds blackbody *radiation*, owing to spectrally sharp emission in surface polaritons. We turn the Casimir-Polder interaction between Cs($7P_{1/2}$) and a sapphire interface into a sensor sharply filtering, at 24.687 THz, the near-field sapphire emission at ∼24.5 THz. The temperature evolution of the sapphire mode is demonstrated. The Cs sensor, sensitive to both dispersion and dissipation, suggests the polariton to be redshifted and sharper, as compared, up to 1100 K, to predictions from far-field sapphire emission, affected by birefringence and multiple resonances.

DOI: 10.1103/PhysRevLett.131.143801

The universality of blackbody radiation (BBR) [1] led to energy quantization for matter and photons, founding the quantum era. BBR applies in the far field (FF) only, with respect to a wavelength $\sim hc/k_BT$ (50 μm for 300 K). At shorter distances [2–5], the contribution of evanescent fields, whose spectral features are material-dependent, dramatically enhances thermal exchanges; similarly, the BBR limit can be beaten for small emitters [6,7]. This near-field (NF) regime opens fascinating applications [4–15], such as smart thermal infrared source (frequency, directivity, high-speed modulation) [16,17], coherent thermal emission controlled by surface engineering (gratings or metafabrication [18–22]), harvesting of thermal energy or refrigeration [23,24], thermal imaging [25–28], and thermal rectification [29–31]. Ultimately, for a "close contact" transfer at atomic scale, distinguishing "radiation" and "conduction" becomes questionable [32–35] because the evanescent field originates in thermally populated *surface polaritons* [36,37], i.e., hybrid particles coupling optical excitation and phonons originating in lattice excitation, hence involving a *phonon* transfer.

Spectral selectivity associated with the narrow-band NF thermal fluctuations [5], which affects both dissipative and dispersive effects, is essential for many applications. However, quantitative evaluations are few, often limited to very specific systems designed for nanothermal engineering [19,22]. Indeed, monitoring thermal exchanges between macroscopic bodies, or stabilizing a temperature difference, is challenging at nanometric distances [10,14]. NF scanning microscopy allows a local probing of the thermal field [25,26,38], but the nanoprobe itself perturbs the polariton spectrum [5,28,39].

The thermal electromagnetic fluctuations are constrained by boundary conditions imposed by surface shape and material properties, so that spatial variations of NF thermal exchanges depend primarily on surface modes, and Maxwell propagation. Hence, for sake of simplicity, we concentrate here on the *complex* surface response for an interface between a planar homogeneous hot material and vacuum, $S(\omega)$:

$$S(\omega) = [\varepsilon(\omega) - 1]/[\varepsilon(\omega) + 1], \tag{1}$$

with $\varepsilon(\omega)$ the macroscopic (relative) permittivity. As a major issue, further discussed, surface resonances occur for $\varepsilon(\omega) \to -1$, far away from bulk resonances [8,40–43].

NF thermal emission is now encompassed in fluctuating electrodynamics [44], which also covers Casimir *dispersion* forces [45,46] describing the macroscopic quantum attraction at short distances between two polarizable neutral bodies. Casimir interaction, originally described for $T = 0$, results from the boundary conditions for vacuum fluctuations. Precision Casimir experiments now test fundamental predictions (standard model or hypothetical non-Newtonian gravity [47–49]), but demand $T \neq 0$ corrections and a realistic material description [50–52]. The analogous "Casimir-Polder" (CP) interaction [53,54] between a neutral surface and a distant atom, benefiting from the intrinsic accuracy of atomic physics, has received various investigations in the very short distance regime–i.e. dipole-dipole van der Waals (vW) interaction. Among achievements, resonant couplings with surface modes [41,55,56], and temperature dependence, were notably demonstrated [57,58].

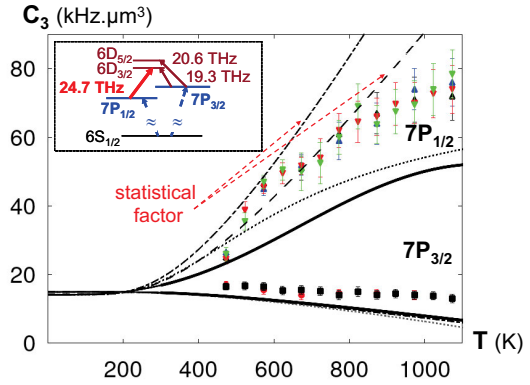

FIG. 1. Experimental evaluations of $C_3(T)$ for Cs($7P$) derived from FM-SR spectroscopy on the $6S_{1/2} \rightarrow \{7P_{1/2}, 7P_{3/2}\}$ doublet (see inset and relevant dipole couplings), and predictions. For the $6S_{1/2} \rightarrow 7P_{1/2}$ transition, the 4 hyperfine components are plotted separately (black triangles: $4 \rightarrow 4$, blue triangles: $4 \rightarrow 3$; red down triangles: $3 \rightarrow 3$, green down triangles: $3 \rightarrow 4$); for the $6S_{1/2} \rightarrow 7P_{3/2}$ transition, black and red squares are, respectively, for the $3 \rightarrow \{2, 3, 4\}$ and $4 \rightarrow \{3, 4, 5\}$ manifolds; Cs reservoir temperature is 180 °C. The dashed and dashed-dotted lines are predictions based upon sapphire permittivity at ~300 K (respectively, [60] and [61]), the dotted ones consider a T-dependent permittivity [62]; the thick ones use our sapphire measurements.

Here, we analyze the narrow NF emission of sapphire (Al_2O_3), a technologically important material, up to $T \sim 1100$ K, by comparing two radically different methods: (i) Through a quasi-coincidence [41,55] between the sapphire surface emission and the Cs $7P_{1/2} \rightarrow 6D_{3/2}$ transition ($\omega_{at}/2\pi = 24.687$ THz, i.e., ~12.15 μm or ~823 cm^{-1} [41,55,56,59]–see inset of Fig. 1), the CP interaction on Cs($7P_{1/2}$) at short distance (~100 nm) narrowly filters the polariton thermal emission at $\omega_p/2\pi \sim$ 24.5 THz (~1200 K) [41,56]. (ii) Alternately, we evaluate surface polariton properties, i.e., $S(\omega)$ from Eq. (1), with $\varepsilon(\omega)$ extrapolated from the broadband FF thermal emission.

In the short distance vW limit, the CP interaction varies as $-C_3.z^{-3}$ (z: atom-surface distance [41,43,57–59]. The interaction, dominated by infrared transition couplings (see Supplemental Material [63]), strongly varies when the thermal emission of the surface polariton (at ω_p) nearly coincides with an *absorption* transition (at ω_{at} —dipole strength D_{at}) [57,58,63], following

$$C_3(T) - C_3(T=0) = -2D_{at}^2.\Re e[S(\omega_{at})].[\exp(\hbar\omega_{at}/k_BT) - 1]^{-1} + o(T). \quad (2)$$

In Eq. (2), the dominant right-hand-side term depends on the thermal Bose-Einstein factor, and on the surface resonant response (*real*, i.e., dispersion) filtered at ω_{at}; the o(T) term, residual for $k_BT \geq \hbar\omega_{at}$, includes the nonresonant dipole couplings, and a D_{at}^2 contribution remaining insensitive to the surface resonance.

To measure C_3, frequency-modulated selective reflection spectroscopy (FM-SR) at a vapor interface is a robust method, probing a typical depth $\sim\lambda_{opt}/2\pi$ [55,56,58,59,87,88]. The measurement results from an optimized fitting of the experimental spectrum, on the basis of a single-parameter family of dimensionless FM-SR spectra [63]. We perform FM-SR on the second resonance doublet of Cs $6S_{1/2} \rightarrow \{7P_{1/2}, 7P_{3/2}\}$ (respectively, $\lambda_{opt} =$ 459 nm, $\lambda_{opt} = 456$ nm) [59]. As a spectroscopic method, FM-SR yields a differential coefficient $\Delta C_3 = [(C_3(|7P\rangle) - C_3(|6S_{1/2}\rangle)]$, here dominated by $C_3(|7P\rangle)$, i.e., $C_3(|7P_{1/2}\rangle)$ or $C_3(|7P_{3/2}\rangle)$ [59]. Cs($7P_{3/2}$) is primarily investigated for comparison purposes, as only coupled to the remote wing of the sapphire polariton—through $7P_{3/2} \rightarrow \{6D_{3/2}, 6D_{5/2}\}$ transitions, respectively, at 19.259 and 20.544 THz, see inset of Fig. 1 and [63].

Figure 1 synthesizes our $C_3(|7P\rangle, T)$ measurements. For Cs($7P_{1/2}$), $C_3(T)$ nearly triples from 500 to 1100 K, while it gently decreases for Cs($7P_{3/2}$). This growth (owing to $\Re e[S(\omega_{at})] < 0$) evidences the *resonant* coupling between Cs($7P_{1/2}$) and sapphire thermal emission. It slows down at high-T: this signs a temperature modification of the surface resonance, i.e., a T dependence for $\Re e[S(\omega_{at}, T)]$; otherwise, $C_3(T)$ should follow the statistical factor of Eq. (2), governing the dashed and dashed-dotted lines (Fig. 1) derived with Eq. (1) for a constant sapphire permittivity—as measured at ambient temperature only [60,61] (see also [89]). Figure 1 also shows predictions (dotted and thick lines) with a T-dependent sapphire permittivity ([43,62,90] and discussion in [63]): as a trend, the agreement with our NF atomic sensor determinations for $C_3(T)$ is better, but remains relative, even for the thick line derived from our own measurements on sapphire windows from the very same origin than the one of the Cs vapor cell (identically superpolished and annealed, see Refs. [58,63]). Ironically, when considering this careful evaluation of $S(\omega_{at}, T)$—detailed below—, the agreement is slightly worse than for predictions (dotted line) considering a permittivity $\varepsilon(\omega, T)$ [62,63] evaluated from measurements limited to the midinfrared transparency region, on sapphire samples of an unknown origin, and modeled with an additional extrinsic resonance.

From FF thermal emission, that we have recorded with a state-of-the-art spectrometer [91], the complex-valued $\varepsilon(\omega, T)$, yielding $S(\omega, T)$, is extracted by fitting [43,63] a modified Lorentz dielectric function model including Gaussian multiphonon contributions *via* self-energy functions (wave number-dependent dampings). Sapphire birefringence adds a touch of complexity: the window at Cs vapor interface is $c_\perp$ (cut perpendicular to the c axis) to ensure the cylindrical symmetry of CP interaction, yielding an effective permittivity $\varepsilon_{eff} = (\varepsilon_o.\varepsilon_e)^{1/2}$ [41,92] (ε_o and ε_e,

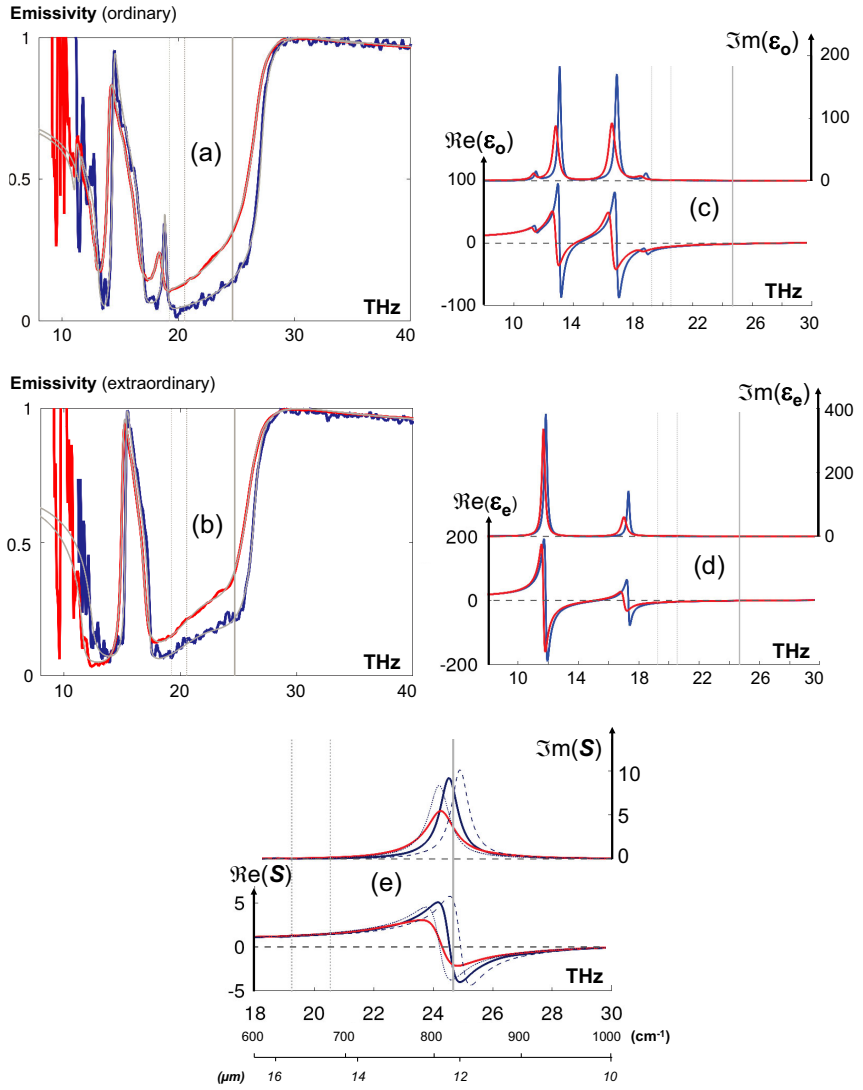

FIG. 2. Sapphire *spectral* response at ~500 (blue), and ~1000 K (red)—for exact temperatures and more details, see Ref. [63]. Experimental emissivity spectrum (reliable above 12 THz, see Ref. [63]), and analytical fittings (black): (a) $c_\perp$ sapphire window, yielding ε_o. (b) $c_{//}$ sapphire window and parallel polarization, yielding ε_e. Relative permittivity $\varepsilon(\omega)$ extrapolated from analytical fits of emissivity: (c) $\varepsilon_o(\omega)$; (d) $\varepsilon_e(\omega)$. (e) Complex surface response $S(\omega)$ calculated for $\varepsilon_{\text{eff}}(\omega) = (\varepsilon_o.\varepsilon_e)^{1/2}$ (full line), along with ~500 K responses $S_o(\omega)$ and $S_e(\omega)$ [from $\varepsilon_o(\omega)$ and $\varepsilon_e(\omega)$] (respectively, dashed and dotted line). Note the additional horizontal scale in cm^{-1}, and μm, provided for convenience. The vertical markers show the dominant couplings: full line for $\text{Cs}(7P_{1/2})$, dotted lines for $\text{Cs}(7P_{3/2})$.

respectively, the ordinary and extraordinary axes permittivity). The number of intrinsic modes is imposed by crystallography, depending on orientation (4 for ordinary, 2 for extraordinary [41,43,60]). Figure 2 exemplifies the measured and calculated emissivity sapphire spectra [Figs. 2(a)–2(b)] for T~500 and $T \sim 1000$ K (more temperatures in [63]). No salient singularities on emissivity [Figs. 2(a)–2(b)] help to locate resonances for $\varepsilon(\omega)$ [Figs. 2(c)–2(d)], or $S(\omega)$ [Fig. 2(e)].

Along with thermal enhancement of CP dispersion forces involving *virtual* atom-surface exchanges, surface thermal emission should induce *real* resonant energy absorption $7P_{1/2} \rightarrow 6D_{3/2}$, with the same z^{-3} spatial dependence [40,57,93]. The reverse $6D_{3/2} \rightarrow 7P_{1/2}$ transfer, analyzed as a Förster-like *quenching* of atomic excitation induced by an absorbing surface mode, had been demonstrated [94], nevertheless without quantitative measurements. We have unsuccessfully attempted to detect directly, as in [94], this $\text{Cs}(7P_{1/2})$ *absorption* of thermal energy, through an induced $\text{Cs}(6D_{3/2})$ population. Rather, we have extended the use of *linear* FM-SR, from the evaluation of the *dispersive* part of the surface interaction, to quantitative information on the *dissipative* exchanges, checking the relative amplitude of the doublet components

$6S_{1/2} \rightarrow 7P_{1/2}, 7P_{3/2}$. No NF thermal energy transfer is expected for $\mathrm{Cs}(7P_{3/2})$, while thermal transfer shortens the $\mathrm{Cs}(7P_{1/2})$ lifetime, specifically implying a spatially-dependent optical width, from γ_∞ in free-space to $\gamma(z) = \gamma_\infty + \Delta\Gamma(T).z^{-3}$, with

$$\Delta\Gamma(T) = 4\, D_{\mathrm{at}}^2.\Im\mathrm{m}[S(\omega_{\mathrm{at}})].[\exp(\hbar\omega_{\mathrm{at}}/k_B T) - 1]^{-1}. \quad (3)$$

This lifetime shortening of $\mathrm{Cs}(7P_{1/2})$, governed by $\Im\mathrm{m}[S(\omega_{\mathrm{at}})]$, follows the same statistical factor as Eq. (2) [63], and the same z^{-3} dependence. The additional spatial dependence $\gamma(z)$ mostly reduces amplitude of FM-SR spectra, complexifying moderately the line shape family with an additional parameter (see Ref. [63]). Inserting our estimates [Fig. 2(e) and [63]] into Eq. (3) yields $\Delta\Gamma(T = 1000\ \mathrm{K}) \sim 40\ \mathrm{kHz}\,\mu\mathrm{m}^3$: the amplitude of the $6S_{1/2}$-$7P_{1/2}$ FM-SR signal should become, at high-T, about twice smaller than for the unaffected $6S_{1/2}$-$7P_{3/2}$ transition (see Fig. 3). Indeed, close to ω_{at}, $\Re\mathrm{e}[S(\omega, T)]$ and $\Im\mathrm{m}[S(\omega, T)]$ evolve nearly parallel above ~500 K, yielding $\Im\mathrm{m}([S(\omega_{\mathrm{at},}, T)]/|\Re\mathrm{e}[S(\omega_{\mathrm{at},}, T)]| \sim 1$–$2$ [63]. Actually, the experimental amplitude ratio (Fig. 3) agrees with $T = 0$ predictions, once standard geometrical ratios for fine and hyperfine components [56,59,95] are included. In view of our measurements accuracy, this implies $\Im\mathrm{m}[S(\omega_{\mathrm{at}})]/|\Re\mathrm{e}S(\omega_{\mathrm{at}})| \leq 0.1$–$0.2$.

The discrepancies between our NF measurements and predictions from FF emissivity fitting cannot be explained by uncertainties affecting temperature measurements, atom dipole couplings, or the $C_3(T)$ evaluation from FM-SR spectra (see Ref. [63]). Rather, relatively to expectations from Fig. 2(e), we suspect the polariton resonance to be sharper and red-shifted, because, close to a surface resonance, $S(\omega)$ is merely a complex Lorentzian [96], with $\Im\mathrm{m}S(\omega)$ and $\Re\mathrm{e}S(\omega)$ associated respectively to absorption and dispersion. Hence, $\Im\mathrm{m}[S(\omega_{\mathrm{at}})]/|\Re\mathrm{e}S(\omega_{\mathrm{at}})| \ll 1$ implies that ω_{at} falls away from the anomalous dispersion region, with the peak amplitude for $S(\omega)$ largely exceeding $\Re\mathrm{e}[S(\omega_{\mathrm{at}})]$; $\Re\mathrm{e}[S(\omega_{\mathrm{at}})] < 0$ confirms that ω_{at} lies in the blue wing of the surface resonance. This hypothetical conclusion appears not incompatible with previous observations benefiting of the same Cs/sapphire coincidence at lower temperatures [63]. A complementary test for sapphire could be offered with $\mathrm{Rb}(7P_{3/2})$, through the dual resonant couplings $7P_{3/2} \rightarrow \{6D_{3/2}, 6D_{5/2}\}$, respectively, at 24.494 and 24.561 THz [56].

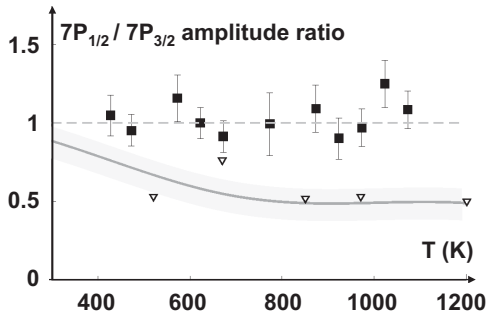

FIG. 3. Temperature dependence of the FM-SR amplitude ratio [$6S_{1/2} \rightarrow 7P_{1/2}$ over $6S_{1/2} \rightarrow 7P_{3/2}$]; amplitudes are normalized to $C_3 = 0$, and to the geometrical factors (fine and hyperfine manifolds [59]). The discrete triangles are predictions evaluated from our $S(\omega, T)$ [Fig. 2(e) and [63]], the thick line is evaluated for $S(\omega, \mathrm{T})$ derived from [62]. The light gray area around the thick line accounts for amplitude ratio dependence with the optical width (central part: $\gamma_\infty = 20$ MHz).

Finally, for $\mathrm{Cs}(7P_{3/2})$, $C_3(T)$ appears slightly above predictions (Fig. 1), here insensitive to the specific modeling of sapphire polariton. This contrasts with the very good agreement found previously for $\mathrm{Cs}(7D_{3/2})$ [58,63], on the same cell, for a very comparable situation. However, the main T-dependent coupling was at 27.7 THz, in the opposite (blue) wing of the polariton, away from the multiple resonances of sapphire polariton. Uncertainties on $S(\omega, T)$ could be more severe for the red wing of ω_{p}, where $\varepsilon_{\mathrm{o}}(\omega)$ and $\varepsilon_{\mathrm{e}}(\omega)$ differ considerably because of birefringence [see Figs. 2(c)–2(d), major resonances respectively at ~13.5 and ~17 THz, vs ~12 THz]. In particular, the major ε_{e} resonance falls partly outside the effective measurement range (~12–60 THz, see Ref. [63]), i.e., $\varepsilon_{\mathrm{e}}(\omega)$ is extrapolated, rather than resulting from a genuine fitting. Additionally, the ε_{e} resonance appears narrower than the two main resonances for ε_{o} [Fig. 2(d)], and this width impacts the remote wing of $\varepsilon_{\mathrm{eff}}$, up to ω_{at}.

To summarize, we demonstrate strong magnification of the CP interaction for $\mathrm{Cs}(7P_{1/2})$ through the resonant coupling to the NF thermally emitted surface polariton. The observed $C_3(T)$, not amenable to Bose-Einstein statistics, evidences a temperature evolution of surface resonance. The FM-SR linearity allows comparing the very different behaviors of the $\mathrm{Cs}(7P)$ doublet components: it reveals unique to provide simultaneously information related to dispersive and dissipative contributions of the surface emission. Predictions classically derived from the fitting of FF thermal emission at high-T for $\Im\mathrm{m}[S(\omega_{\mathrm{at}})]$ disagree with FM-SR measurements, so that we suspect the actual surface resonance to be sharper than expected and slightly redshifted. This discrepancy also appears with alternate descriptions of bulk sapphire properties: extrapolation of FF emission to the surface resonance is fragile, and here, birefringence and sapphire multiple resonances bring extra difficulties.

Our results tackle the issue, of a general interest, of accuracy when evaluating surface mode resonances and NF spectral emission. Aside from the large shift between surface and bulk resonances, extrapolating $\varepsilon(\omega, \mathrm{T})$ from broadband FF emissivity (or reflectance) [43,60,63] is intrinsically delicate as the complex-valued permittivity has to be derived from a real-valued spectral measurement. This is permitted by the Kramers-Kronig relationship but

requires in the principle to know the entire spectrum. Classically, on a limited spectral range (5–25 μm in our case), a "guessed" analytical shape is optimized for permittivity, leading to a variety of sets of fitting parameters. The resulting ambiguity induces only negligible effects for $\varepsilon(\omega)$ and $S(\omega)$ in our modeling [63]. However, all models imply hard-to-test assumptions to describe the very remote wings of $\varepsilon(\omega)$ resonance, essential for evaluating $S(\omega_p)$. This would make valuable a direct measurement of the complex refractive index, in the range of the expected surface resonance. Ellipsometry is appropriate for this purpose, but remains underdeveloped in the infrared range and at high-T. The few corresponding measurements rely mostly on "spectroscopic ellipsometry," based upon an *a priori* description of the permittivity (see, e.g., [61,97]).

Even if we have restricted ourselves to the extreme NF regime, and to thermal exchanges where one of the "materials" (Cs) is a narrow filter ideally known, uncertainties issues for surface resonances remain extremely relevant for longer distances, or for nanostructured interfaces—including exchanges between two-dimensional layered materials [98]. Indeed, unexpected surface responses were often observed [25], evoking complex mechanisms, including non local response [99], strain [60], hot electrons within colder phonon vibrations [100], local glass structure instead of a crystalline one [101], along with chemical residuals [102,103]. Here, the consistency of fitting FM-SR spectra with a z^{-3} potential is confirmed, in a regime dominated by the surface thermal emission: this makes very credible that Cs atoms effectively interact with a neutral surface; oppositely, when deriving $\varepsilon(\omega)$ from reflectance measurement, ideal "bulk" homogeneity and local planarity are implicit, ignoring issues of atomistic surface reorganization [104] or low-dimensionality [105].

Evaluating accurately NF thermal emission, including surface resonances, should benefit to various prospects: (i) In Casimir research, oversimplified models describing material properties (e.g., Drude vs plasma [106]) lead to known discrepancies: literature and tabulated data (e.g., [107]) should be scrutinized critically. For CP interaction, NF material properties will govern the fine temperature tuning, turning vW attraction into repulsion, see, e.g., [43]. (ii) Converting thermal surface emission into a quantized excitation (here, the unobserved $7P_{1/2} \rightarrow 6D_{3/2}$ absorption) would open exciting possibilities [108,109], among which selective thermal NF population of molecular vibration modes (e.g. SiC surface modes at 28.5 THz coincide with NH_3 or SF_6 vibrations): this "surface thermal pumping" would ultimately generate specific (non "Boltzmann") internal energy distributions. (iii) Birefringence, which notably affects sapphire, but SiC too, is shown here to induce dramatic changes of thermal infrared emission bands with orientation [110]. Engineering NF thermal conductivity, isolation, or rectification by orientating microbodies from the same material [10], appears exciting: presently, predicting the orientation dependence of surface resonances remains challenging [111].

We thank D. Sarkisyan and his group (Ashtarak, Armenia) for the fabrication of the high-T Cs vapor cell. The stay of J. C. de A. C. was supported by the Brazilian grant *Ciências sem Fronteiras*. Various steps of this work were enriched with frequent discussions with J. R. Rios Leite, H. Failache, M. Chevrollier, M. Oriá, T. Passerat de Silans, and P. Echegut. We also acknowledge discussions on near-field thermal emission and measurements with J-J. Greffet and Y. de Wilde, We also acknowledge the suggestions of the referees, and the advice of J-M. Raimond, for editing the manuscript. This research triggered support by the MITI interdisciplinary program of CNRS ("xNF High-T emission").

*Corresponding author: daniel.bloch@univ-paris13.fr
†Present address: Departamento de Física, Universidade Federal de Pernambuco, Recife, PE 50670-901, Brazil.
‡Permanent address: Centro de Educação e Saúde, Universidade Federal de Campina Grande, 581750-000 Cuité, PB, Brazil.

[1] M. Planck, On the law of the energy distribution in the normal spectrum, Ann.Phys. (Berlin) **309**, 553 (1901).
[2] S. Rytov, *Theory of Electric Fluctuations and Thermal Radiation* (Academy of Sciences Press, Moscow, 1953); translation in AFCRC-TR-59-162 (1959), https://apps.dtic.mil/sti/pdfs/AD0226765.pdf.
[3] D. Polder and M. Van Hove, Theory of radiative heat transfer between closely spaced bodies, Phys. Rev. B **4**, 3303 (1971).
[4] A. V. Shchegrov, K. Joulain, R. Carminati, and J-J. Greffet, Near-Field Spectral Effects due to Electromagnetic Surface Excitations, Phys. Rev. Lett. **85**, 1548 (2000).
[5] A. Babuty, K. Joulain, P-O. Chapuis, J-J. Greffet, and Y. de Wilde, Black-Body Spectrum Revisited in the Near Field, Phys. Rev. Lett. **110**, 146103 (2013).
[6] C Wuttke and A. Rauschenbeutel, Thermalization via Heat Radiation of an Individual Object Thinner than the Thermal Wavelength, Phys. Rev. Lett. **111**, 024301 (2013).
[7] D. Thompson, L. Zhu, R. Mittapally, S. Sadat, Z. Xing, P. McArdle, M. M. Qazilbash, P. Reddy, and E Meyhofer, Hundred-fold enhancement in far-field radiative heat transfer over the blackbody limit, Nature (London) **561**, 216 (2018).
[8] K. Joulain, J-P. Mulet, F. Marquier, R. Carminati, and J.-J. Greffet, Surface electromagnetic waves thermally excited: Radiative heat transfer, coherence, properties and Casimir forces revisited in the near field, Surf. Sci. Rep. **57**, 59 (2005).
[9] S. Basu, Z. M. Zhang, and C. J. Fu, Review of near-field thermal radiation and its application to energy conversion, Int. J. Energy Res. **33**, 1203 (2009).

[10] R. S. Ottens, V. Quetschke, S. Wise, A. A. Alemi, R. Lundock, G. Mueller, D. H. Reitze, D. B. Tanner, and B. F. Whiting, Near-Field Radiative Heat Transfer between Macroscopic Planar Surfaces, Phys. Rev. Lett. **107**, 014301 (2011).

[11] O. D. Miller, S. G. Johnson, and A. W. Rodriguez, Shape-Independent Limits to Near-Field Radiative Heat Transfer, Phys. Rev. Lett. **115**, 204302 (2015).

[12] S. Fan, Perspective: Thermal photonics, and energy applications, Joule **1**, 264 (2017).

[13] K. Kim, B. Song, V. Fernández-Hurtado, W. Le, W. Jeong, L. Cui, D. Thompson, J. Feist, M. T. H Reid, F J. García-Vidal, J. C. Cuevas, E. Meyhofer, and P. Reddy, Radiative heat transfer in the extreme near field, Nature (London) **528**, 387 (2015).

[14] B Song, D. Thompson, A. Fiorino, Y. Ganjeh, P. Reddy, and E. Meyhofer, Radiative heat conductances between dielectric and metallic parallel plates with nanoscale gaps, Nat. Nanotechnol. **11**, 509 (2016).

[15] S.-A. Biehs, R. Messina, P. S. Venkataram, A. W. Rodriguez, J. C. Cuevas, and P. Ben-Abdallah, Near-field radiative heat transfer in many-body systems, Rev. Mod. Phys. **93**, 025009 (2021).

[16] F. Marquier, K. Joulain, J.-P. Mulet, R. Carminati, J.-J. Greffet, and Y. Chen, Coherent spontaneous emission of light by thermal sources, Phys. Rev. B **69**, 155412 (2004).

[17] S. Vassant, I. Moldovan Doyen, F. Marquier, F. Pardo, U. Gennser, A. Cavanna, J. L. Pelouard, and J. J. Greffet, Electrical modulation of emissivity, Appl. Phys. Lett. **102**, 081125 (2013).

[18] J-J. Greffet, R. Carminati, K. Joulain, J-P. Mulet, S. Mainguy, and Y. Chen, Coherent emission of light by thermal sources, Nature (London) **416**, 61 (2002).

[19] K. Ikeda, H. T. Miyazaki, T. Kasaya, K. Yamamoto, Y. Inoue, K. Fujimura, T. Kanakugi, M. Okada, K. Hatade, and S. Kitagawa, Controlled thermal emission of polarized infrared waves from arrayed plasmon nanocavities, Appl. Phys. Lett. **92**, 021117 (2008).

[20] X. Liu, T. Tyler, T. Starr, A. F. Starr, N. M. Jokerst, and W. J. Padilla, Taming the Blackbody with Infrared Metamaterials as Selective Thermal Emitters, Phys. Rev. Lett. **107**, 045901 (2011).

[21] R. St-Gelais, L. Zhu, S. Fan, and M. Lipson, Near-field radiative heat transfer between parallel structures in the deep subwavelength regime, Nat. Nanotechnol. **11**, 515 (2016).

[22] A. C. Overvig, S. A. Mann, and A. Alù, Thermal Metasurfaces: Complete Emission Control by Combining Local and Nonlocal Light-Matter Interactions, Phys. Rev. X **11**, 021050 (2021).

[23] G. Jaliel, R. K. Puddy, R. Sánchez, A. N. Jordan, B. Sothmann, I. Farrer, J. P. Griffiths, D. A. Ritchie, and C. G. Smith, Experimental Realization of a Quantum Dot Energy Harvester, Phys. Rev. Lett. **123**, 117701 (2019).

[24] S. Buddhiraju, W. Li, and S. Fan, Photonic Refrigeration from Time-Modulated Thermal Emission, Phys. Rev. Lett. **124**, 077402 (2020).

[25] A. Kittel, W. Müller-Hirsch, J. Parisi, S-A. Biehs, D. Reddig, and M. Holthaus, Near-Field Heat Transfer in a Scanning Thermal Microscope, Phys. Rev. Lett. **95**, 224301 (2005).

[26] Y. de Wilde, F. Formanek, R. Carminati, B. Gralak, P.-A. Lemoine, K. Joulain, J.-P. Mulet, Y. Chen, and J.-J. Greffet, Thermal radiation scanning tunnelling microscopy, Nature (London) **444**, 740 (2006).

[27] L. Worbes, D. Hellmann, and A. Kittel, Enhanced Near-Field Heat Flow of a Monolayer Dielectric Island, Phys. Rev. Lett. **110**, 134302 (2013).

[28] D. Halbertal, J. Cuppens, M. Ben Shalom, L. Embon, N. Shadmi, Y. Anahory, H. R. Naren, J. Sarkar, A. Uri, Y. Ronen, Y. Myasoedov, L. S. Levitov, E. Joselevich, A. K. Geim, and E. Zeldov, Nanoscale thermal imaging of dissipation in quantum systems, Nature (London) **539**, 407 (2016).

[29] B. Li, L Wang, and G. Casati, Thermal Diode: Rectification of Heat Flux, Phys. Rev. Lett. **93**, 184301 (2004).

[30] C. R. Otey, W. T. Lau, and S. Fan, Thermal Rectification through Vacuum, Phys. Rev. Lett. **104**, 154301 (2010).

[31] K. Joulain, Y. Ezzahri, J. Drevillon, B. Rousseau, and D. de Sousa Meneses, Radiative thermal rectification between SiC and SiO_2, Opt. Express **23**, A1388 (2015).

[32] D. G. Cahill, P. V. Braun, G. Chen, D R. Clarke, S. Fan, K. E. Goodson, P. Keblinski, W. P. King, G. D. Mahan, A. Majumdar, H. J. Maris, S. R. Phillpot, E. Pop, and L. Shi, Nanoscale thermal transport. II. 2003–2012, Appl. Phys. Rev. **1**, 011305 (2014).

[33] G. Domingues, S. Volz, K. Joulain, and J.-J. Greffet, Heat Transfer between Two Nanoparticles Through Near Field Interaction, Phys. Rev. Lett. **94**, 085901 (2005).

[34] K. Kloppstech, N. Könne, S. Biehs, A. W. Rodriguez, L. Worbes, D. Hellmann, and A. Kittel, Giant heat transfer in the crossover regime between conduction and radiation, Nat. Commun. **8**, 14475 (2017).

[35] K. Y. Fong, H-K. Li, R. Zhao, S. Yang, Y. Wang, and X. Zhang, Phonon heat transfer across a vacuum through quantum fluctuations, Nature (London) **576**, 243 (2019).

[36] Surface polaritons: Electromagnetic waves at surfaces and interfaces, *Modern Problems in Condensed Matter Sciences*, edted by V. M. Agranovich and D. L. Mills (Elsevier, New York, 1982), Vol. 1.

[37] D. N. Basov, M. M. Fogler, and F. J. García de Abajo, Polaritons in van der Waals materials, Science **354**, aag1992 (2016).

[38] B. T. O'Callahan and M. B. Raschke, Laser heating of scanning probe tips for thermal near-field spectroscopy and imaging, APL Photonics **2**, 021301 (2017).

[39] S. Edalatpour, V. Hatamipour, and M. Francoeur, Spectral redshift of the thermal near field scattered by a probe, Phys. Rev. B **99**, 165401 (2019).

[40] J. M. Wylie and J. E. Sipe, Quantum Electrodynamics near an interface II, Phys. Rev. A **32**, 2030 (1985).

[41] M. Fichet, F. Schuller, D. Bloch, and M. Ducloy, van der Waals interactions between excited-state atoms and dispersive dielectric surfaces, Phys. Rev. A **51**, 1553 (1995).

[42] S. Saltiel, D. Bloch, and M. Ducloy, A tabulation and critical analysis of the wavelength-dependent dielectric image coefficient for the interaction exerted by a surface onto a neighbouring excited atom, Opt. Commun. **265**, 220 (2006).

[43] T. Passerat de Silans, I. Maurin, P. Chaves de Souza Segundo, S. Saltiel, M-P Gorza, M. Ducloy, D. Bloch, D. de Sousa Meneses, and P. Echegut, Temperature

dependence of the dielectric permittivity of CaF_2, BaF_2 and Al_2O_3: application to the prediction of a temperature-dependent van der Waals surface interaction exerted onto a neighbouring $Cs(8P_{3/2})$ atom, J. Phys. Condens. Matter **21**, 255902 (2009).

[44] E. M. Lifshitz, The theory of molecular attractive forces between solids, Sov. Phys. JETP **2**, 73 (1956).

[45] H. B. G. Casimir, On the attraction between two perfectly conducting plates, Kon. Ned. Akad. Wetensch. Proc. **51**, 793 (1948).

[46] K. A. Milton, *The Casimir Effect: Physical Manifestations of Zero-Point Energy* (World Scientific, Singapore, 2001).

[47] R. S. Decca, D. López, E. Fischbach, G. L. Klimchitskaya, D. E. Krause, and V. M. Mostepanenko, Precise comparison of theory and new experiment for the Casimir force leads to stronger constraints on thermal quantum effects and long-range interactions, Ann. Phys. (Amsterdam) **318**, 37 (2005); and also: Tests of new physics from precise measurements of the Casimir pressure between two gold-coated plates, Phys. Rev. D **75**, 077101 (2007).

[48] D. M. Harber, J. M. Obrecht, J. M. McGuirk, and E. A. Cornell, Measurement of the Casimir-Polder force through center-of-mass oscillations of a Bose-Einstein condensate, Phys. Rev. A **72**, 033610 (2005).

[49] I. Antoniadis, S. Baessler, M. Büchner, V. Fedorov, S. Hoedl, A. Lambrecht, V. Nesvizhevsky, G. Pignol, K. Protasov, S. Reynaud, and Yu. Sobolev, Short-range fundamental forces, C. R. Phys. **12**, 755 (2011).

[50] A. O. Sushkov, W. J. Kim, D. A. R. Dalvit, and S. K. Lamoreaux, Observation of the thermal Casimir force, Nat. Phys. **7**, 230 (2011).

[51] A. Canaguier-Durand, P. A. Maia Neto, A. Lambrecht, and S. Reynaud, Thermal Casimir effect for Drude metals in the plane-sphere geometry, Phys. Rev. A **82**, 012511 (2010).

[52] S. de Man, K. Heeck, R. J. Wijngaarden, and D. Iannuzzi, Halving the Casimir Force with Conductive Oxides, Phys. Rev. Lett. **103**, 040402 (2009).

[53] H. B. G. Casimir and D. Polder, The influence of retardation on the London-van der Waals forces, Phys. Rev. **73**, 360 (1948).

[54] Yu. S. Barash and V. L. Ginzburg, Expressions for the energy density and evolved heat in the electrodynamics of a dispersive and absorptive medium, Sov. Phys. Usp. **19**, 263 (1976).

[55] H. Failache, S. Saltiel, M. Fichet, D. Bloch, and M. Ducloy, Resonant van der Waals Repulsion Between Excited Cs Atoms and Sapphire Surface, Phys. Rev. Lett. **83**, 5467 (1999).

[56] H. Failache, S. Saltiel, M. Fichet, D. Bloch, and M. Ducloy, Resonant coupling in the van der Waals interaction between an excited alkali atom and a dielectric surface an experimental study via stepwise spectroscopy, Eur. Phys. J. D **23**, 237 (2003).

[57] M-P. Gorza and M. Ducloy, van der Waals interactions between atoms and dispersive surfaces at finite temperature, Eur. Phys. J. D **40**, 343 (2006).

[58] A. Laliotis, T. Passerat de Silans, I. Maurin, M. Ducloy, and D. Bloch, Casimir-Polder interactions in the presence of thermally excited surface modes, Nat. Commun. **5**, 4364 (2014).

[59] M. Chevrollier, M. Fichet, M. Oria, G. Rahmat, D. Bloch, and M. Ducloy, High resolution selective reflection spectroscopy as a probe of long-range surface interaction: measurement of the surface van der Waals attraction exerted on excited Cs atoms, J. Phys. II (France) **2**, 631 (1992).

[60] A. S. Barker, Infrared lattice vibrations and dielectric dispersion in corundum, Phys. Rev. **132**, 1474 (1963).

[61] M. Schubert, T. E. Tiewald, and C. M. Herzinger, Infrared dielectric anisotropy and phonon modes of sapphire, Phys. Rev. B **61**, 8187 (2000).

[62] M. E. Thomas, S. K. Andersson, R. M. Sova, and R. I. Joseph, Frequency and temperature dependence of the refractive index of sapphire, Infrared Phys. Technol. **39**, 235 (1998).

[63] See Supplemental Material at http://link.aps.org/supplemental/10.1103/PhysRevLett.131.143801, for Cs atom properties and predictions of its interaction with a thermally excited surface, for the experimental analysis for evaluation of surface interaction by atomic spectroscopy, and for measurements and interpretation of sapphire emissivity, and occurrences of Refs. [66–88].

[64] A. Kramida, Yu. Ralchenko, J. Reader, and NIST ASD Team, *NIST Atomic Spectra Database* (ver. 5.10). [Online]., Available: https://physics.nist.gov/asd [2023, March 23]. (National Institute of Standards and Technology, Gaithersburg, MD, 2022).

[65] M. S. Safronova, U. I. Safronova, and C. W. Clark, Magic wavelengths, matrix elements, polarizabilities, and lifetimes of Cs, Phys. Rev. A **94**, 012505 (2016).

[66] O. S. Heavens, Radiative transition probabilities of the lower excited states of the alkali metals, J. Opt. Soc. Am. **51**, 1058 (1961).

[67] A. Lindgård and S. E. Nielsen, Transition probabilities for the alkali isoelectronic sequences Li I, Na I, K I, Rb I, Cs I, Fr I, At. Data Nucl. Data Tables **19**, 612 (1977).

[68] A. N. Nesmeyanov, *Vapor Pressure of the Chemical Elements* (Elsevier, Amsterdam, 1963).

[69] J. M. Obrecht, R. J. Wild, and E. A. Cornell, Measuring electric fields from surface contaminants with neutral atoms, Phys. Rev. A **75**, 062903 (2007).

[70] J. M. McGuirk, D. M. Harber, J. M. Obrecht, and E. A. Cornell, Alkali-metal adsorbate polarization on conducting and insulating surfaces probed with Bose-Einstein condensates, Phys. Rev. A **69**, 062905 (2004).

[71] J. C. de Aquino Carvalho, I. Maurin, H. Failache, D. Bloch, and A. Laliotis, Velocity preserving transfer between highly excited atomic states: Black body radiation and collisions, J. Phys. B **54**, 035203 (2021).

[72] G. Toh, D. Antypas, and D. S. Elliott, Measurement of the Stark shift of the $6s^2S_{1/2} \rightarrow 7p^2P_J$ transitions in atomic cesium, Phys. Rev. A **89**, 042512 (2014).

[73] A. M. Akul'shin, V. L. Velichanskii, A. S. Zibrov, V. V. Nikitin, V. A. Sautenkov, E. K. Yurkin, and N. V. Senkov, Collisional broadening of intra-Doppler resonances of selective reflection on the D_2 line of cesium, JETP Lett. **36**, 303 (1982), https://ui.adsabs.harvard.edu/abs/1982ZhPmR..36..247A/abstract.

[74] N. Papageorgiou, M. Fichet, V. A. Sautenkov, D. Bloch, and M. Ducloy, Doppler-free reflection spectroscopy of self-induced and krypton-induced collisional shift and

broadening of Cesium D_2 line components in optically dense vapor, Laser Phys. **4**, 392 (1994).
[75] M. Fichet, F. Schuller, D. Bloch, and M. Ducloy, Interaction de van der Waals résonnante entre un atome dans un état excité et une surface diélectrique: spectres de réflexion sélective, Ann. Phys. Fr. **20**, 649 (1995).
[76] T. Passerat de Silans, A. Laliotis, I. Maurin, M.-P. Gorza, P. Chaves de Souza Segundo, M Ducloy, and D. Bloch, Experimental observations of temperature effects in the near-field regime of the Casimir–Polder interaction, Laser Phys. **24**, 074009 (2014); see also T. Passerat de Silans, Ph.D. thesis, Paris13 University, 2009, https://tel.archives-ouvertes.fr/file/index/docid/583140/filename/these-Passerat_de_Silans.pdf.
[77] J. C. de Aquino Carvalho, P. Pedri, M. Ducloy, and A. Laliotis, Retardation effects in spectroscopic measurements of the Casimir-Polder interaction, Phys. Rev. A **97**, 023806 (2018).
[78] D. Raskin and P. Kusch, Interaction between a neutral atomic or a molecular beam and a conducting surface, Phys. Rev. **179**, 712 (1969).
[79] W. Lukosz and R. E. Kuhn, Light emission by magnetic and electric dipoles close to a plane interface: I Total radiated power, J. Opt. Soc. Am. **67**, 1607 (1977).
[80] F. Le Kien and A. Rauschenbeutel, Spontaneous emission of a two-level atom with an arbitrarily polarized electric dipole in front of a flat dielectric surface, Phys. Rev. A **93**, 043828 (2016).
[81] P. Todorov, J. C. de Aquino Carvalho, I. Maurin, A. Laliotis, and D. Bloch, Search for deviations from the ideal Maxwell-Boltzmann distribution for a gas at an interface, Proc. SPIE Int. Soc. Opt. Eng. **11047**, 110470P (2019).
[82] A. Laliotis, I. Maurin, M. Fichet, D. Bloch, M. Ducloy, N. Balasanyan, A. Sarkisyan, and D Sarkisyan, Selective reflection spectroscopy at the interface between a calcium fluoride window and Cs vapour, Appl. Phys. B **90**, 415 (2008).
[83] M. R. K. Kelly-Gorham, B. M. DeVetter, C. S. Brauer, B. D. Cannon, S. D. Burton, M. Bliss, T. J. Johnson, and T. L. Myers, Complex refractive index measurements for BaF_2 and CaF_2 via single-angle infrared reflectance spectroscopy, Opt. Mat. **72**, 743 (2017).
[84] J. F. Brun, L. del Campo, D. de Sousa Meneses, and P. Echegut, Infrared optical properties of α-alumina with the approach to melting: γ-like tetrahedral structure and small polaron conduction, J. Appl. Phys. **114**, 223501 (2013).
[85] A. K. Harman, S. Ninomiya, and S. Adachi, Optical constants of sapphire (α-Al_2O_3) single crystals, J. Appl. Phys. **76**, 8032 (1994).
[86] R. M. Sova, M. J. Linevsky, M. E. Thomas, and F. F. Mark, High-temperature infrared properties of sapphire, AlON, fused silica, yttria, and spinel, Infrared Phys. Technol. **39**, 251 (1998).
[87] M. Ducloy and M. Fichet, General theory of frequency modulated selective reflection: Influence of atom surface interactions, J. Phys. II (France) **1**, 1429 (1991).
[88] D. Bloch and M. Ducloy, Atom-wall interaction in *Advances in Atomic, Molecular and Optical Physics*, edited by B. Bederson and H. Walther (Elsevier Academic, New York, 2005), Vol. 50, pp. 91–154, 10.1016/S1049-250X(05)80008-4.
[89] F. Gervais, Aluminum Oxide (Al_2O_3), in *Handbook of Optical Constants of Solids II*, edited by E. D. Palik (Academic, San Diego, 1991), pp. 761-775; W. J. Tropf and M. E. Thomas, Aluminum Oxide (Al_2O_3) Revisited, in *Handbook of Optical Constants of Solids III*, edited by E. D. Palik (Academic, San Diego, 1998), pp. 653–682.
[90] J.C de Aquino Carvalho, Ph.D. thesis, Paris13 University, 2018, https://tel.archives-ouvertes.fr/tel-01886223.
[91] D. de Sousa Meneses, P. Melin, L. del Campo, L. Cosson, and P. Echegut, Apparatus for measuring the emittance of materials from far infrared to visible wavelengths in extreme conditions of temperature, Infrared Phys. Technol. 2015) 96 ,**69**).
[92] M.-P. Gorza, S. Saltiel, H. Failache, and M. Ducloy, Quantum theory of van der Waals interactions between excited atoms and birefringent dielectric surfaces, Eur. Phys. J. D **15**, 113 (2001).
[93] H. Failache, Ph.D. thesis, Paris13 University, 1999.
[94] H. Failache, S. Saltiel, A. Fischer, D. Bloch, and M. Ducloy, Resonant Quenching of Gas-Phase Cs Atoms Induced by Surface Polaritons, Phys. Rev. Lett. **88**, 243603 (2002).
[95] D. Antypas and D. S. Elliott, Measurement of the radial matrix elements of the $6s^2S_{1/2} \rightarrow 7p^2P_J$ transitions in atomic cesium, Phys. Rev. A **88**, 052516 (2013).
[96] J. C de Aquino Carvalho and D. Bloch, Surface response around a sharply resonant surface polariton mode is simply a Lorentzian, Opt. Lett. **46**, 2876 (2021).
[97] J. Y. Yang, W. J. Zhang, and L. H. Liu, Anisotropic dielectric functions of (0001) sapphire from spectroscopic ellipsometry and first-principles study, Physica (Amsterdam) **473B**, 35 (2015).
[98] S. A. Dereshgi, T. G. Folland, A. A. Murthy, X. Song, I. Tanriover, V. P. Dravid, J. D. Caldwell, and K. Aydin, Lithography-free IR polarization converters via orthogonal in-plane phonons in α-MoO_3 flakes, Nat. Commun. **11**, 5771 (2020).
[99] F. Singer, Y. Ezzahri, and K. Joulain, Near field radiative heat transfer between two nonlocal dielectrics, J. Quant. Spectrosc. Radiat. Transfer **154**, 55 (2015).
[100] Y. Dubi and Y. Sivan, "Hot" electrons in metallic nanostructures—nonthermal carriers or heating?, Light Sci. Appl. **8**, 89 (2019).
[101] M. Simoncelli, N. Marzari, and F. Mauri, Unified theory of thermal transport in crystals and glasses, Nat. Phys. **15**, 809 (2019).
[102] L Cui, W. Jeong, V. Fernandez-Hurtado, J. Feist, F. J. Garcia-Vidal, J. C. Cuevas, E. Meyhofer, and P. Reddit, Study of radiative heat transfer in Ångström and nanometre-sized gaps, Nat. Commun. **8**, 14479 (2017).
[103] A. Schlaich, E. W. Knapp, and R. R. Netz, Water Dielectric Effects in Planar Confinement, Phys. Rev. Lett. **117**, 048001 (2016).
[104] G. Binnig, H. Rohrer, C. Gerber, and E. Weibel, 7×7 Reconstruction on Si(111) Resolved in Real Space, Phys. Rev. Lett. **50**, 120 (1983).
[105] S. Lepria, R. Livi, and A. Politi, Thermal conduction in classical low-dimensional lattices, Phys. Rep. **377**, 1 (2003).

[106] M. Hartmann, G.-L. Ingold, and P. A. Maia Neto, Plasma versus Drude Modeling of the Casimir Force: Beyond the Proximity Force Approximation, Phys. Rev. Lett. **119**, 043901 (2017).

[107] *Optical Handbook of the Optical Constants of Solids*, edited by E. Palik (Academic Press, New York, 3 volumes [vol. I: (1985), vol. II: (1991), vol. III: (1998)].

[108] A. Canaguier-Durand, E. Devaux, J. George, Y. Pang, J. A. Hutchison, T. Schwartz, C. Genet, N. Wilhelms, J.-M. Lehn, and T. W. Ebbesen, Thermodynamics of molecules strongly coupled to the vacuum field, Angew. Chem., Int. Ed. **52**, 10533 (2013).

[109] A. Thomas, L. Lethuillier-Karl, K. Nagarajan, R. M. A. Vergauwe, J. George, T. Chervy, A. Shalabney, E. Devaux, C. Genet, J. Moran, and T. W. Ebbesen, Tilting a ground state reactivity landscape by vibrational strong coupling, Science **363**, 615 (2019).

[110] K. F. Young and H. P. R. Frederikse, Compilation of the static dielectric constant of inorganic solids, J. Phys. Chem. Ref. Data **2**, 313 (1973).

[111] S. E. Kim, F. Mujid, A. Rai, F. Eriksson, J. Suh, P. Poddar, A. Ray, C. Park, E. Fransson, Y. Zhong, D. A. Muller, P. Erhart, D. G. Cahill, and J. Park, Extremely anisotropic van der Waals thermal conductors, Nature (London) **597**, 660 (2021).